column to beam ${}_cM_u/{}_bM_u$ (No.9,16,17,18).

Shear Stress versus Shear Distortion in Joint

Figure 7 shows the shear stress versus shear distortion in joints. Comparing Fig.7 with Fig.6, the following interesting tendency can be noticed. For the specimens whose failure mode is BY-BF, the increase of shear distortion due to repeated loading is very small and is limited to 0.8% at the most ultimate (No.1,2,7,8,10,16). On the contrary, for the specimens whose failure mode is BY-JS, the shear distortion passes over 0.8% at earlier loading stage, and then increases rapidly, and the hysteresis loop of Fig.6 shows pinching corresponding to that of Fig.7. Even for specimens whose final failure mode is BY-JS, the hysteresis loops retain spindle, as long as their distortion is less than 0.8%.

Test Variables and Failure Modes

Figure 8 shows the relationship between the final failure modes and the three test variables such as column axial level σ_o, hoop content ratio p_w, and intermediate column reinforcement ratio K, where K is defined as follows;

$$K = \frac{\text{cross sectional area of intermediate column bars}}{\text{total cross sectional area of column bars}} \qquad (1)$$

With increase of the value of every variable, the failure mode changes from joint shear failure to beam flexural failure. There certainly exists a correlation between the failure modes and these variables.

DUCTILITY ESTIMATION

Quantification of Critical Cumulative Ductility Factor

From the above consideration of the test results, it was clarified that the confinement of the joint, and consequently the aseismic performance of beam-column subassemblages, became more favorable with increase of column axial force, joint hoop content, and intermediate column bars. The increase of moment resisting capacity of columns was also effective to increase the aseismic ability. If these parameters can be presented as a continuous quantity, it may be useful for aseismic design of beam-column joints. The authors paid attention to the critical value ${}_{E}\rho_{C}$ of cumulative displacement ductility factor defined as the axis of abscissa in Fig.5, at which the joint shear distortion reached 0.8% as shown in Fig.7. The experimental values of ${}_{E}\rho_{C}$ of each specimen are shown in Table 3, and these values are small for BY-JS type and large for BY-BF type. Based on the test results, the critical value ρ_{C} was newly quantified as a linear function of four test variables, with a simple regression method, as follows;

$$\rho_{C} = 2.38 + 177\sigma_{0} + 38.6p_{w} + 20.7K - 5.00\eta \qquad (2)$$

where, σ_{0} : column axial stress level, $N/(A_{C}\ f_{C}')$
p_{w} : hoop content ratio (%)
K : intermediate column bar ratio defined as Eq.(1)
η : ${}_{b}M_{u}/{}_{c}M_{u}$

Calculated values of ρ_{C} from Eq.(2) agree fairly with those from the experiments as shown in Fig.9, in which two points for one specimen are plotted because of counting the positive and negative loadings independently. Fig.9 represents or substantiates the tendency considered qualitatively in Fig.6,7 and 8. It may be conceived that specimens fail in joint shear for $\rho_{C} \leqq 30$, and fail in beam flexure for $\rho_{C} > 30$.

Comparisons with other Investigations

In order to ascertain the effectiveness of Eq.(2), the calculated values of ρ_{C} of other investigators' exterior beam-column joint tests in Japan were plotted in Fig.10. The number of sampling data is about 60, and the references of the adopted data are shown precisely in the authors paper (5). The abscissa in Fig.10 was the development length L_{h} of beam bars in joint divided by barthe diameter d_{b}. It can be seen that Eq.(2) is also effective to distinguish whether the failure mode is BY-JS type or BY-BF type, provided that the value of L_{h}/d_{b} is greater than 12.

CONCLUSIONS

Reversed cyclic loading tests of eighteen exterior beam-column subassemblages were carried out. Column axial force, amount of joint hoop reinforcement, existence of intermediate bars and moment resisting capacity of columns were selected as experimental variables. On the basis of thorough consideration of the test results, the following major remarks were obtained:

1. The ratio of shear stress at yielding of beam to shear strength in joint was designed less than 0.5 for every specimens.

Nevertheless, ten of eighteen specimens failed due to joint shear under the repetition of reversed loading following yielding of the beams.

2. Ductility of subassemblages increases with the increase in the column axial compressive force and amount of joint hoop reinforcement, while the tensile axial force reduces the ductility remarkably. Existence of intermediate column bars is also effective to increase the ductility.

3. The critical cumulative displadement ductility factor, at which the value of joint shear distortion reaches 0.8%, was quantified as a function of the experimental variables, and was ascertained to be very effective in estimating the aseismic performance of exterior beam- column subassemblages.

ACKNOWLEDGMENT

This research formed a part of the investigation on "Mechanical behavior of exterior beam-column joint in RC frame" represented by Prof. Morita,S.,Kyoto University, and received the grant in aid for scientific research from the Ministry of Education, Japan. The tests were carried out successfully through Aoki,M. and Sano,Y.'s efforts who were Master course students of Toyohashi University of Technology. The authors would like to thank all of them.

REFERENCES

1. Kamimura,T.,"Ultimate Shear Strength of R/C Beam-Column Joint", Summary of Annual Meeting of AIJ,1975,pp.1155-1156.

2. Teraoka,M. et'al,"Study on the Behavior of R/C Interior Beam -Column Joint", Summary of Annual Meeting of AIJ, Vol.C,1986, pp.115-116

3. Kanata,K., Fujii,S. and Morita,S.,"Effects of Joint Shear Reinforcement on Behavior of Exterior Beam-Column Joint under Reversed Cyclic Loading",Transactions of the JCI, Vol.7,1985, pp.559-566

4. Kaku,T.,"Effect of Bent-Bar Anchorage on the Behavior of Exterior Beam-Column Joint", 8th Conference of JCI,1986, pp.641-644

5. Kaku,T., Asakusa,H. and Aoki,M.,"Ductility Estimation of Exterior Beam-Column Subassemblages in Reinforced Concrete Frames", Transactions of AIJ,Journal of Structural and Engrg., No.401,1989,pp.87-96

Table 1 Properties of Test Specimens

Group	No	Specimen	Concrete Comp. fc' (MPa)	Concrete Ten. (MPa)	Column Main Bar	Column Main Bar Ag (mm^2)	Column Axial Load N (KN)	Column Axial Load $\frac{N}{Ac \cdot fc'}$	Joint Hoop	Joint Hoop Pw (%)	Moment capacity $_cM_u$	Moment capacity $_bM_u$	Moment capacity $_cM_{bu}$	Moment capacity $\frac{_cM_{bu}}{_cM_u}$	Shear stress $_p\tau_{by}$	Shear stress $_p\tau_u$	Shear stress $\frac{_p\tau_{by}}{_p\tau_u}$
1	1	4D16·H6+17	31.1	2.3	4D16	796	258	0.17	R6	0.49	48.6	37.8	18.2	0.38	4.11	9.64	0.43
	2	4D16·H6+10	41.7	2.9			199	0.10			45.5	38.5	18.5	0.41	4.16	9.64	0.43
	3	4D16·H6+00	41.7	2.6			0	0.0			27.6	38.2	18.4	0.67	4.14	9.64	0.43
	4	4D16·H3+17	44.7	3.6			360	0.17	R3	0.12	58.4	37.7	18.2	0.31	4.06	8.75	0.46
	5	4D16·H3+09	36.7	2.9			160	0.09			42.5	37.5	18.1	0.43	4.06	8.75	0.46
	6	4D16·H3+00	40.4	2.9			0	0.0			27.5	38.4	18.5	0.67	4.15	8.75	0.47
2	7	4D10·8D10·H6+12	32.2	3.2	12D10	856	194	0.12	R6	0.49	46.9	37.8	18.2	0.39	4.11	9.64	0.43
	8	4D10·8D10·H6+08	41.2	3.3			160	0.08			46.7	37.8	18.2	0.39	4.08	9.64	0.42
	9	4D10·8D10·H6+00	40.6	3.2			0	0.0			32.8	37.8	18.2	0.56	4.08	9.64	0.42
	10	4D10·8D10·H3+17	44.4	3.5			360	0.17	R3	0.12	59.7	37.7	18.2	0.30	4.06	8.75	0.46
	11	4D10·8D10·H3+08	41.9	2.6			160	0.08			47.3	37.7	18.2	0.38	4.07	8.75	0.47
	12	4D10·8D10·H3+00	35.1	2.6			0	0.0			33.0	37.9	18.3	0.55	4.11	8.75	0.47
	13	4D10·8D10·H6-04	46.4	3.1			-100	-0.04	R6	0.49	23.5	38.3	18.4	0.79	4.13	9.64	0.43
3	14	4D13·8D06·H3+08	41.0	3.4	4D13, 8D6	764	160	0.08	R3	0.12	40.6	37.7	18.2	0.45	4.07	8.76	0.47
	15	4D13·4D10·H3+08	39.7	3.1	4D13, 4D10	793	160	0.08			44.3	37.6	18.1	0.41	4.06	8.75	0.46
4	16	4D13·8D13·H6+00	37.4	2.7	12D13	1524	0	0.0	R6	0.49	54.6	37.7	18.2	0.33	4.08	9.64	0.42
	17	4D10·8D06·H6+00	39.7	2.8	4D10, 8D6	541	0	0.0			18.4	38.2	18.4	1.00	4.14	9.64	0.43
	18	4D06·8D06·H6+00	40.7	2.9	12D6	384	0	0.0			11.1	37.2	17.9	1.61	4.02	9.64	0.42

Beam Main bar: Upper=4-D13(508mm^2,1.56%), Lower=4-D13(508mm^2,1.56%)

Ancharage: Radius of bend = 40mm(3d), Horizontally projected length = 195mm(15d), Tail length = 143mm(11d).

$_cM_u$: Moment capacity of column(KN·m). $_bM_u$: Moment capacity of beam(KN·m). $_cM_{bu}$: Bending moment of column at $_bM = {}_bM_u$(KN·m).

$_p\tau_{by}$: Shear stress in joint at $_bM = {}_bM_y$ (MPa).

$_p\tau_u$: Shear stress calculated by Kamimura's Eq. ; $(0.82-0.02f_c')f_c' + p_w \cdot {}_s\sigma_y$ (MPa).

Table 2 Mechanical Properties of Test Bars

Bar	Yield Point (MPa)	Max.Strength (MPa)	Elongation (%)
D16	360	541	25.3
D13(Beam)	391	594	23.4
D13	381	553	25.5
D10	395	564	22.9
D6	282	468	27.9
R6	250	537	28.9
R3	281	365	—

Table 3 Test Results and Critical Cumulative Ductility Factors

No	Name	Qy	δy	Qmax	Mode	$_E\rho_c$	σ_o	Pw	K	η	ρ_c
1	4D16•H6+17	42.0	8.04	54.1	BY→BF	46.1 49.3	0.189 0.153	.494	0.00	0.75 0.81	51.1 44.5
2	4D16•H6+10	42.4	8.26	54.6	BY→BF	34.2 50.5	0.112 0.086	.494	0.00	0.81 0.89	37.2 32.2
3	4D16•H6+00	43.4	11.71	47.4	BY→JS	9.4 11.0	0.012 -0.011	.494	0.00	1.29 1.50	17.1 12.0
4	4D16•H3+17	42.4	8.44	52.2	BY→JS	29.8 27.4	0.178 0.155	.124	0.00	0.63 0.67	35.5 31.3
5	4D16•H3+09	38.9	7.99	48.2	BY→JS	17.2 16.0	0.103 0.077	.124	0.00	0.84 0.93	21.2 16.2
6	4D16•H3+00	42.1	12.71	45.7	BY→JS	3.0 2.0	0.012 -0.011	.124	0.00	1.30 1.50	2.8 -2.3
7	4D10•8D10•H6+12	40.9	8.13	54.3	BY→BF	34.9 58.4	0.142 0.108	.494	0.50	0.78 0.88	53.0 46.7
8	4D10•8D10•H6+08	41.8	8.15	53.2	BY→BF	53.7 49.8	0.092 0.068	.494	0.50	0.78 0.84	44.2 39.6
9	4D10•8D10•H6+00	39.7	9.51	51.5	BY→JS	13.0 18.0	0.012 -0.012	.494	0.50	1.08 1.24	28.5 23.5
10	4D10•8D10•H3+17	43.0	8.50	53.0	BY→BF	40.1 37.5	0.179 0.156	.124	0.50	0.62 0.65	46.1 41.9
11	4D10•8D10•H3+08	41.4	7.91	50.4	BY→JS	28.7 29.5	0.090 0.067	.124	0.50	0.77 0.83	29.6 25.2
12	4D10•8D10•H3+00	40.3	8.62	45.3	BY→JS	10.1 11.6	0.013 -0.013	.124	0.50	1.08 1.22	14.4 9.1
13	4D10•8D10•H6-04	41.3	12.27	45.7	BY→JS	2.9 2.0	-0.034 -0.053	.494	0.50	1.49 1.77	18.3 13.6
14	4D13•8D06•H3+08	41.7	8.83	49.3	BY→JS	24.5 22.7	0.092 0.068	.124	0.20	0.89 0.98	23.2 18.4
15	4D13•4D10•H3+08	41.9	8.49	50.3	BY→JS	25.9 31.6	0.096 0.074	.124	0.22	0.81 0.88	24.6 20.4
16	4D13•8D13•H6+00	41.4	8.88	54.8	BY→BF	53.5 30.8	0.011 -0.014	.494	0.50	0.67 0.72	30.4 25.7
17	4D10•8D06•H6+00	37.2	9.66	38.5	CY→JS	7.0 8.3	0.008 -0.008	.494	0.31	1.93 2.25	19.6 15.2
18	4D06•8D06•H6+00	23.1	4.71	26.0	CY→CF	29.7 19.3	0.005 -0.006	.494	0.50	3.10 3.72	17.2 12.1

Qy: Load at beam bar yielding(KN). δy: Displacement at Qy(mm). Qmax: Maximum load(KN).

Failure mode "BY → BF": Flexural failure in beam after yielding of beam bars.
"BY → JS": Shear failure in joint after yielding of beam bars.
"CY → JS": Shear failure in joint after yielding of column bars.
"CY → CF": Flexural failure in column after yielding of column bars.

$_E\rho_c$: Experimental critical cumulative ductility factor,
at which shear distortion reaches γ=0.008.

ρ_c : Critical cumulative ductility factor calculated by Eq.(2).

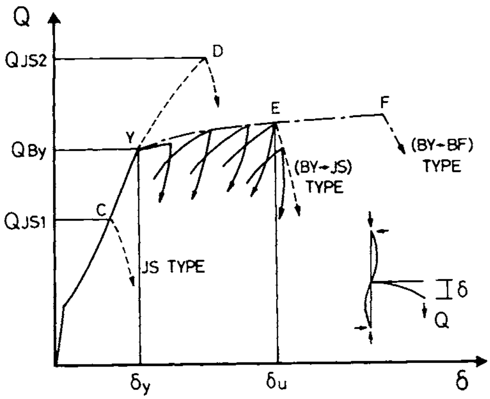

Fig. 1--Ductility evaluation of a beam-column subassemblage

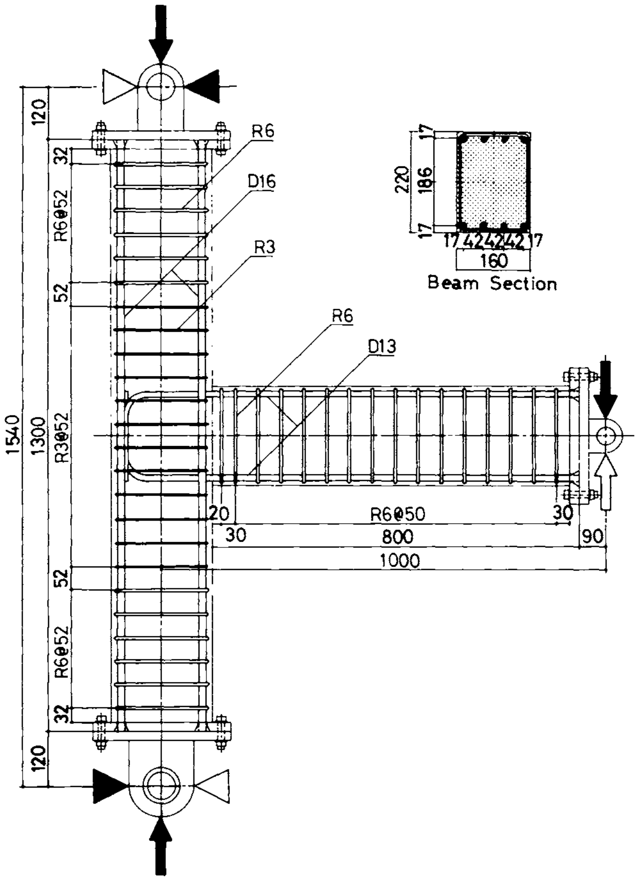

Fig. 2--Dimensions and reinforcement of test specimens

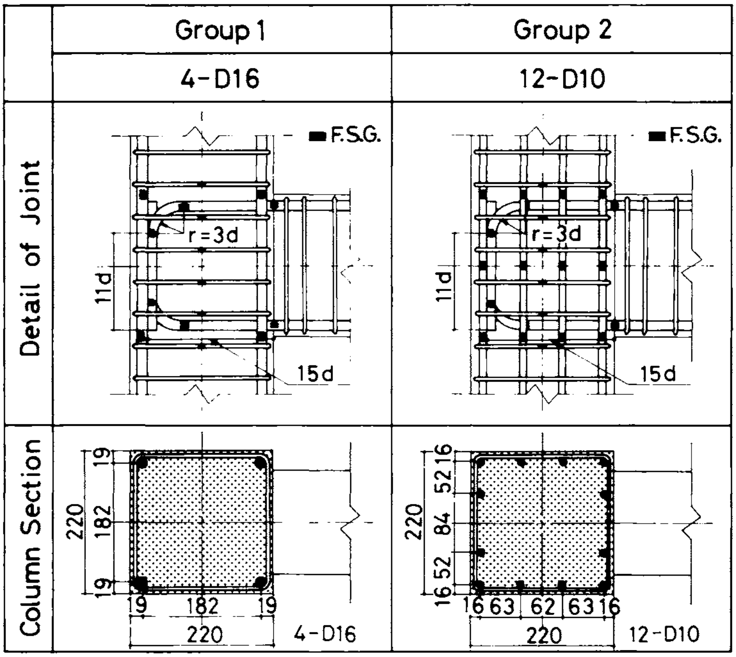

Fig. 3--Reinforcing details in the joint

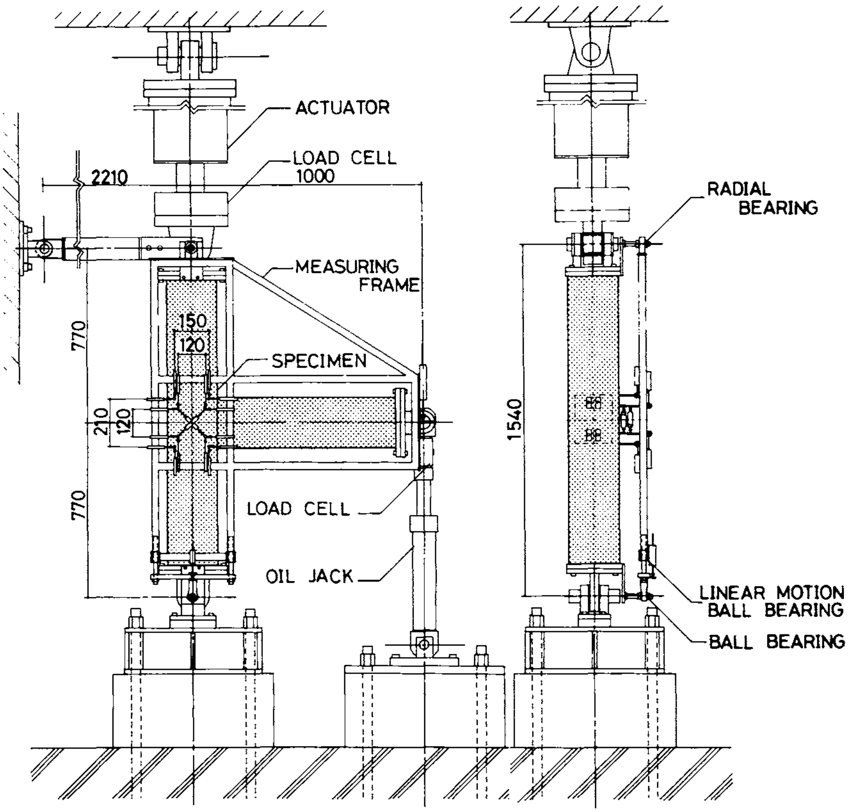

Fig. 4--Loading set up and measuring instrumentations

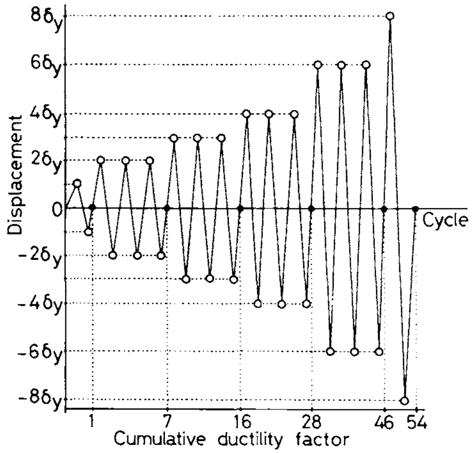

Fig. 5--Imposed displacement during loading runs

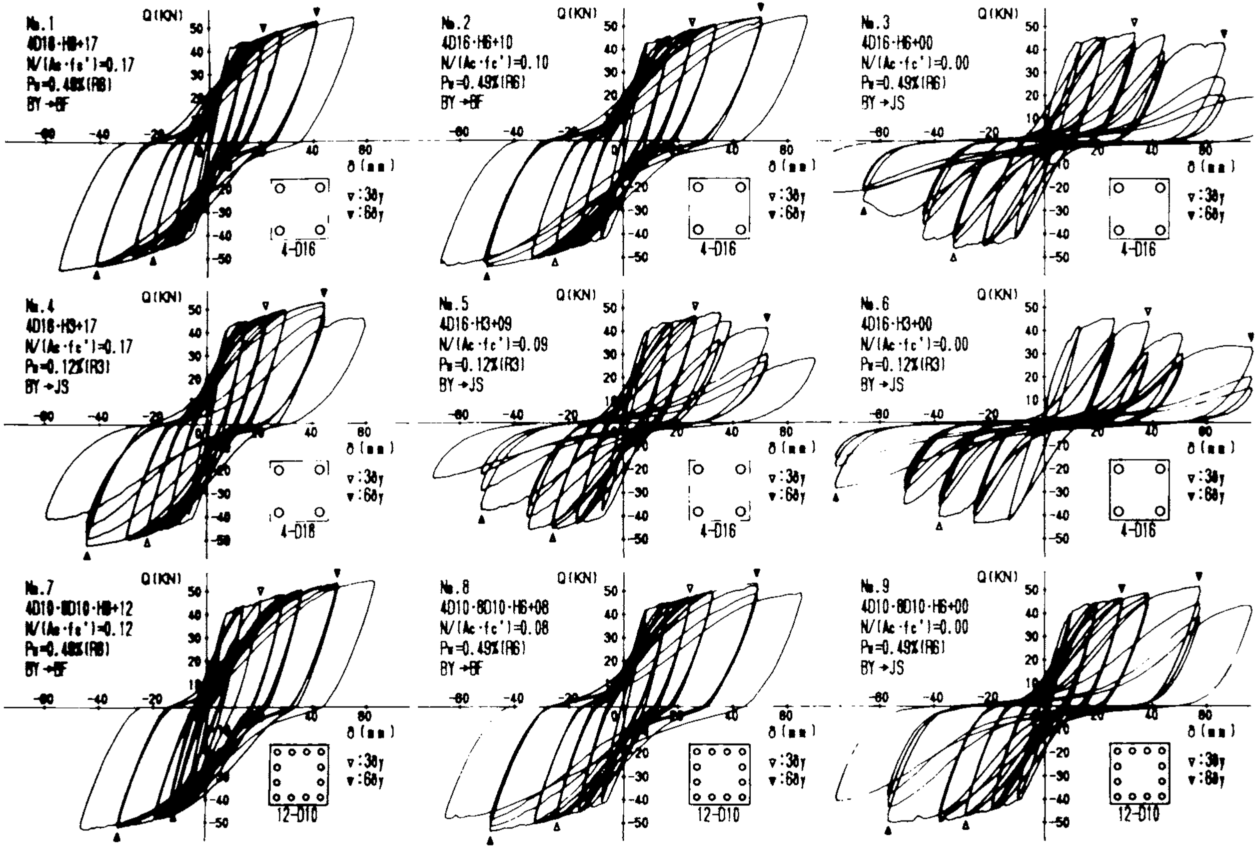

Fig. 6--Beam shear force -- story drift curves